Transformation of a Piston Engine into a Compressed Air Engine with Rotary Valve

M. Akif Kunt*
Dumlupinar University Tavsanli Vocational Training School, Assistant Professor,
Dept. of Motor Vehicles and Transportation Technology &, Kutahya, Turkey

Abstract

Compressed air engines, compressed air using piston-cylinder engine mechanism design is an alternative that can be obtained on the job. In this study, a four cycle- single cylinder, internal combustion engine has been transformed into a pneumatic engine with rotary valve operating according to two cycle engine principle due to per unit time more power. Performance tests made of fixed working pressure, different engine loads in exhaust valve timing ExOA 20°. At the ExOA 20^o exhaust valve timing 25 bar working pressure, engine speed of 800 rpm were obtained 17.28 Nm engine torque, 1.48 kW engine power and maximum motor efficiency 24.42%.

Keywords— *compressed air engine, low emission engines, air-breathing engines, two-stroke engines*

.

I. INTRODUCTION

The engines, which operate on the basis of expansion created by a compressed gas liquid on the piston, are called pneumatic engine. Especially due to the advantages like inexpensiveness and environment-friendly structure, pneumatic and cryogenic power systems have found usage in over populated areas such as parks, stadiums, covered garages, etc. [1-5]. In addition, power/weight ratios and filling costs of pneumatic systems are low. [6-7]. Pioneering work in the area of the compressed air engine has been done by French technologist Guy and Cyril [8] and also by an inventor of quasi turbine Saint Hilaire et al. [9]. Use of compressed air as working fluid offers a prime mover which does not involve a combustion process for producing shaft work. Thus, the great advantages in terms of availability of air as fuel and the emissions free from carbon dioxide, carbon monoxide, and nitrous oxides are apparent to such air motors. Compressed air driven prime-movers are also found to be cost effective compared to fossil-fuel-driven engines. It has the perennial compressed air requirement which needs some source of energy for running compressor whose overall analysis shows that the compressed air system is a quite good option for light vehicle applications [10].

Besides engines driven by compressed air engines, studies have also been made on air engines with hybrid compression. P. Higelin, I. Vasile, A Charlet ve Y. Chamaillard realized the application of air drive with hybrid compression in a diesel engine with direct injection. In experimental studies made, a high pressure air reservoir and a connected filling valve have been placed upon the cylinder head of engine. An additional electrically-driven camshaft has been made for the filling valve. [11]. In the engine, tested in accordance with New European Driving Cycle (NEDC), total energy consumption has been found as 22,4 MJ, effective energy has been found as 2,10 MJ, re-gained braking energy has been found as 0,46 kJ and total cycling output has been found as 9,38%.

Detailed study has been carried out about multi vane expander for its various parameters such as: geometry, end friction, optimizing the efficiency [12–21], and pneumatic hybrid power system [22–25]. The work of pressure regulation of turbine, performance efficiency of Rankine cycle, multistage turbine compressor models, experimental investigation on rotary vane expander, three-stage expander into a CO_2 refrigeration system, end face friction of the revolving vane mechanism, and design and implementation of an air powered motorcycle have also been reviewed [26–27].

The MDI Company in France has realized the design, manufacture, and application of air powered car [28-29]. The engines of compressed air cars are piston type, vane type, rotary type and so on, and the piston engine is widely taken now.

A Koca, R. Bayındır, H. Gunes, M.A. Kunt, S. Sakar have been designed for valve mechanism on a compressed air engine. Mechanical valve mechanism has been removed and a special designed electromagnetic solenoid has been placed. The solenoid that provides the transfer of compressed air to engine has been controlled by driving circuit related to the speed of the engine. According to the simulation results, the wire diameter and the armature mass have a measurable effect on response time [30]. Gunes has converted a two-stroke internal combustion engine of 40cc with a piston and single cylinder into a pneumatic engine by using an electro-magnetic linear valve. The electromagnetic valve has not performed well due to insufficient saturation reached by the coil in high engine cycles. With respect to the highest efficiency of pneumatic engine, engine moment has been found as 3.74 Nm, engine power has been found as 313,1 W, engine efficiency has been found as 19,78% when the operating pressure is 20 bar, opening period of intake valve is 60° and engine speed is 1000 1/min. Moreover, because of the unloading made by two-stroke engines from the port, the expansion after the filling of cylinder reduces very much [31].

II. PNEUMATIC ENGINE CONCEPT

Various cycle graphics are available which can be applied in relation to the pneumatic engines. The valve timings of engine have been determined according to the cycle graphic whose cycle function is maximal when such graphics have been analysed. Figure 2.1 displays a p-V diagram of the pneumatic engine cycle. The timing of the charging valve means that it is open from points 1 to 3. The pressure in the cylinder can be increased by discharging the air tank between points 1 and 2. The position at point can be varied by choosing the timing of the charging valve closure. The expansion, from points 3 to 4 with the charging valve closure, will produce torque to the crankshaft. Eventually, the air will be expelled from the exhaust pipe (from points 4-5-1)

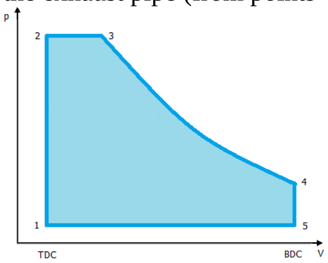

Figure 2.1 Theoretical P-V Diagram Of Pneumatic Engine [11]

A. Rotary Valve Mechanism

Rotary valve has been preferred due to the reasons that it can operate at high pressure to take the compressed air into the cylinder; it can be assembled to the engine easily; it can produced easily; and it causes less friction loss. AISI 410 has been used as rotary cycle material as it has high efficiency in machining manufacturing operations and grinding works, and as it is easy to provide. For rotating valve shaft, mercury steel has been used (according to **DIN** 17006: 115 Cr V3). It has been aimed to make the operating space between rotating valve shaft and valve body 0,01 mm. Lubrication has been applied between shaft and body; bronze bushing has been made into the body in order to prevent leakages. After boring, honing has been applied delicately onto bushing surface in order to integrate bronze bushing and shaft. In order to make shaft remain still against axial forces and pushing in rotary valve mechanism, a segment channel has been bored in the edge of the shaft. In order to decrease the occurrence of leakage to sump of engine from ring walls during applying compressed air on the piston, lap type teflon rings have been used. The valve mechanism has been sized, produced and put to sealing and flow rate tests, on the basis of maximum power of gasoline engine. Figure 2.2 shows the rotary valve mechanism.

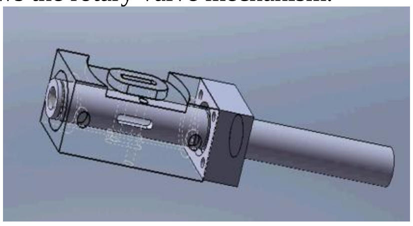

Figure 2.2 Rotary valve mechanism

B. Exhaust Cam Shaft

It is a 20 mm diameter solid shaft. The shaft is supported on two ball bearings staged in their housing and linked with the output shaft of the engine via chain and supported. Figure 2.3 shows the exhaust cam shaft mechanism.

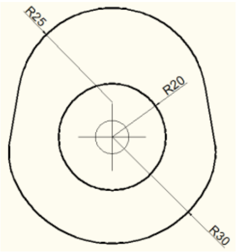

Figure 2.3 Exhaust Cam Shaft

C. Inlet and Exhaust Valve Timing

The converted compressed air engine has been tested for a set of an exhaust valve timings ExOA 20^o. The exhaust cam gives a lift of 6 mm to the follower. When the piston is at TDC the rotary valve is at opened condition and as the compressed air starts entering into the chamber, the valve has to close after 60 degrees after TDC. When the piston is at before 20 degrees BDC, the exhaust valve is at opened condition and the exhaust air starts discharge into atmosphere. For the next 200 degree rotation of the crank, exhaust valve is kept at fully opened condition. Figure 2.4 shows inlet and exhaust valve timing.

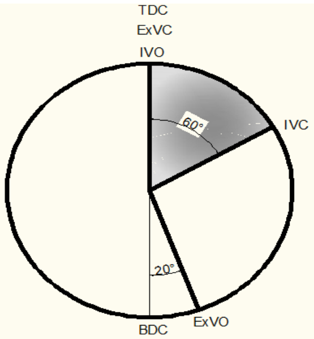

Figure 2.4 Inlet And Exhaust Valve Timing

III. MATERIAL AND METHOD

The process of transforming the engine into a compressed air engine has been carried out in

Faculty of Technology of Gazi University; construction illustrations of valve mechanisms have been drawn and produced. In this study, performance tests have been carried out by transforming a four-stroke internal combustion engine with a piston into a pneumatic engine functioning according to the principle of two-stroke engine. A rotary valve mechanism has been used as the inlet valve system of compressed air engine; and camshaft exhaust mechanism has been used as the exhaust system. The performance tests of compressed air engine have been carried out at fixed operating pressure (25 bar) and different engine loads.
Technical specifications related to the test engine are displayed in the Table 1.

Table 1. Test Engine Specifications

Parameters	Specification
Engine type	4-stroke,OHC,
Bore x Stroke	Φ 88 x 64 mm
Cylinder volume	389 cm^3
Rated power	8,3kW @ 3600 rpm (gasoline)
Maximum torque	26,5 N m/3000 rpm (gasoline)
Compression ratio	8/1
Fuel consumption (g/kW-h)	≤ 395
Cooling mode	Air cooling

A. Experimental Apparatus

As shown in Figure 3.1, the engine load was measured by a lining-type dynamometer with a strain gauge load cell sensor. Accuracy of the dynamometer is 0,003 Nm. Engine speed was measured by a digital tachometer, ENDA ETS1410, with 1 rpm accuracy. In order to measure the amount of air delivered to the system, a flow-meter with metallic tube float (Bass Instrument BF300 type) has been used. Linear measurement precision of the flow-meter, fed by a supply voltage of 24 volt, is 1%. In order to analyze pressure changes within the cylinder in test engine, AVL (QC34C) pressure sensor has been used in test mechanism. Measurement range of pressure sensor is between 0-250 bars, its sensitivity is 20 pC/bar and linearity is • ±0,2 % FSO. For recognition of TDP, an optical encoder, which has (Opkon MRIE 50) TTL outlet, voltage supply of 5V DC and operating speed of 5000 1/min, has been used. National Instrument USB–6259 data collection card has 12V power supply, USB connection and digital transducer resolution. During experiments, pressure signals obtained from the pressure sensor have been passed through amplifier and accordingly the intensity of signal has been increased; then, such signals have been transmitted through data collection card and recorded into the computer. The amplifier used (KISTLER 5015A), has a measuring range of □ ±2…2200000 pC and frequency range of 0…200 kHz and accuracy of < ±%3. Recorded raw data are converted into graphics by means of a programme of sensor company. The encoder used is recorded in data collection card in every 0,36 degree per each pressure data.

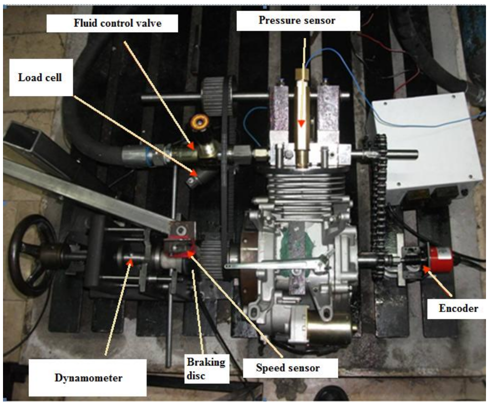

Figure 3.1 Photograph of the Experimental Setup

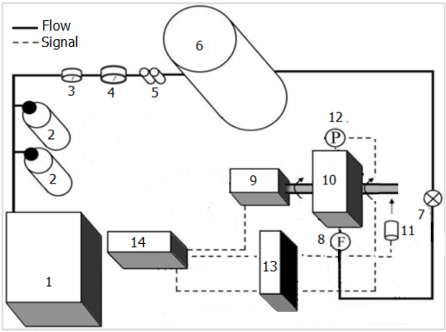

1. Compressor, 2. High pressure tank, 3. High pressure regulator, 4. Low pressure regulator, 5. Water filter, 6. Buffer tank, 7. Flow control valve, 8. Flow meter, 9. Engine dynamometer, 10. Engine, 11. Encoder, 12. Cylinder pressure sensor, 13. Amplifier, 14. DAQ

Figure 3.2 Experimental Setup of the Compressed Air Engine Test Bench

IV. EXPERIMENTAL RESULTS AND EVALUATIONS

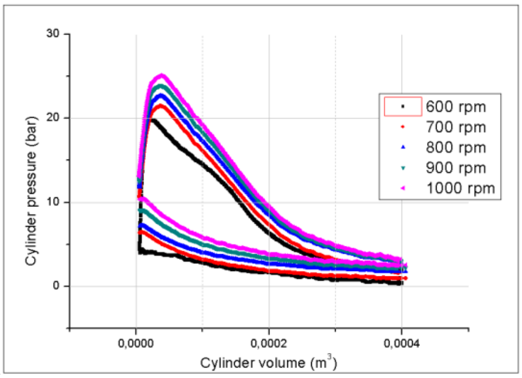

Figure 4.1 P-V Diagram At Exoa 20° Exhaust Valve Timing, 25 Bar Working Pressure For Different Engine Speeds

Figure 4.1 has been provided for the most efficient exhaust valve timing and operating pressure obtained by the engine under all test conditions. When the graphic is examined, it is seen that intra-cylinder maximum pressures decrease while the negative functioning inside the cylinder decreases if engine load is increased as of the engine speed of 900 rpm. This situation is related to the speed of piston. Although the valve duration remains fixed, movement rate of piston within the cylinder decreases as the engine speed decreases. Accordingly, during the realization of exhaust time, efflux of compressed exhaust liquid inside the cylinder becomes easier. In line with the increase in the amount of efflux exhaust liquid, the negative pressure decreases.

Figure 4.2 shows the changing of engine torque, air consumption and engine power depending on engine speed at 25 bar operating pressure and ExOA 20^o exhaust valve timing. When the change in engine torque with respect to the engine speed, it is observed that the engine torque has increased as of 1000 rpm until 800 rpm, and at the engine speed of 600 rpm the engine torque has decreased. Such change shows that filling efficiency inside the engine is the highest at the engine speed of 800 rpm. When loading continues after the engine speed of 800 rpm, it is seen that the engine torque decreases due to increasing leakage. When the change in engine power with respect to the engine speed is analysed, it is observed that if the engine speed is accelerated as of the engine speed of 600 rpm the engine power increases as per functioning amount carried out in the unit of time. It is estimated that the engine power decreases due to frictions and unloading problems at the engine speed higher than this one, in which the engine power tends to reach the maximum point towards the engine speed of 1000 rpm. Maximum engine power is measured as 1.72 kW at 1000 rpm. The highest air consumption is measured 12.4 m^3/h at the engine speed of 600 rpm under test conditions. The cause of maximum air consumption (600 rpm) is air leaks due to cold engine oil and rings.

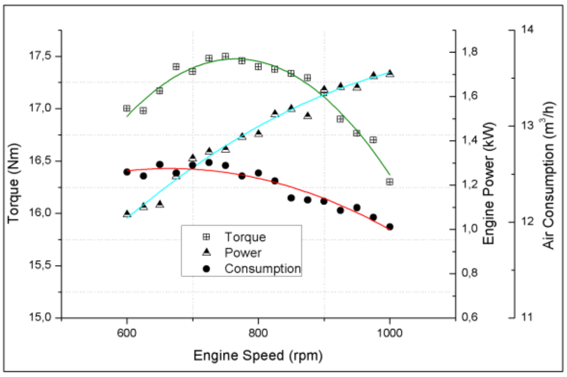

Figure 4.2 Changing of Engine Torque and Engine Power Depending on Engine Speed at 25 Bar Working Pressure, Exoa 20^o Exhaust Valve Timing.

V. CONCLUSIONS

When the performance of pneumatic engines has been compared with the performance of internal combustion engines, it has been observed that the compressed air engines provide higher engine torque and engine power at low engine speed. Average intra-cycle pressure or the compressed air engines is higher than the pressure of internal combustion engines. Therefore, the compressed air engines are a good alternative for the first movement of engines and low vehicle speeds. It is possible to refill the compressed air tubes during the cruise by using the regenerative breaking system of the related vehicle.

The pressure increases as of the conveyance of compressed air into the cylinder; and with the effect of expansion, intra-cylinder pressure decreases after the pressure point. An amount pressure increase occurs inside the cylinder while the piston moves from Top Dead Centre (TDC) towards Bottom Dead Centre (BDC). The reason of such negative pressure increase inside the cylinder is the sole use of compressed air as an energy liquid in order to obtain mechanical energy in compressed air engines. Air consumption of compressed air engines is far more than the air consumption of ordinary engines. Therefore, this exhaust system, which resembles the exhaust system of four-stroke internal combustion engines, cannot perform the sufficient unloading in such engines.

The highest efficiency of the engine has been measured as % 24,42 at the engine speed of 800 rpm, 25 bars operating pressure and ExOA 20^o exhaust valve timing. Furthermore, at this operating point, the engine generates an engine torque of 17,28 Nm and an engine power of 1,48 kW. Maximum engine power is measured as 1.72 kW at 1000 rpm. The highest air consumption is measured 12.4 m^3/h at the engine speed of 600 rpm under test conditions. While determining the efficiency of air engines, reduction of the compression energy of air transferred to the system is highly important.

REFERENCES

[1] Plummer MC.,Ordonez CA., Reidy RF., “A Rewiew of Liquid Nitrogen Propelled Vehicle Programs in the USA, Bulletin of the Kharkov National Automobile and Highway University, Ukraina, 2000, Vol. 12, 13. P. 47-52.

[2] Turenko AN., Pyatak AI., Kudryavtsev IN., Timchenko II., Jadan PV., “Ecologically Clean Cryogenic Transport: Modern State of Problem, Ukraina, 2000, Automobile Transport Vol. 12, 13. P. 42-47.

[3] Turenko AN., Pyatak AI., Kudryavtsev IN., Timchenko II., Jadan PV., “Pneumatic Power Plants for Ecologically Clean Transport Vehicles, Ukaina, Automobile Transport 2001, Vol. 7. 8. P. 193-197.

[4] Bogomolov VA., Kudryavtsev IN., Pyatak AI., Bondarenko SI. Plummer MC., “Development of The New Croyogenic Technologies for Prospective Kinds of Automobile Transport”, Ukraina, Automobile Transport, 2003, Vol. 12. P. 5-7.

[5] Kudryavtsev IN., Kulik AP., Plummer MC., Pyatak I., Tochtar, GI., “Croyogenic Vehicle-Nonpolluting Vehicle for Cities”, Int. Conf., Trasport Ecology-stable

Development, ECO VARNA, Varna, Bulgaria, May 15-17, 2003.
[6] Martin HR., Mcloy D., "The Control of Fluid Power", London, 1-187 (1973).
[7] Pandian SR., "Control Performance of an Air Motor", International Conference on Robotics and Automation, Detroit, 518-524, (1999).
[8] Guy N., Cyril N., "Compressed Air—the Most Sustainable Energy Carrier for Community Vehicles," Speech in front of assembly at Kultur gathered for Fuel CellsWorld 2004.
[9] Saint Hilaire G., Saint Hilaire R., Saint Hilaire Y., "Quasiturbine Zero Pollution Car Using Gasoline", Festival at Le Lundi, Montreal Gazette, September 2005.
[10] Singh BR. Singh O., "Development of a Vaned Type Novel Air Turbine," International Journal of Mechanical Engineering.
[11] Higelin P., Vasile I., Charlet A., Chamaillard Y., "Parametric Optimization of Hybrid Pneumatic–Combustion Engine Concept", Int. J. Eng. Res., 5 (2):205–217 (2003).
[12] Badr O., O'Callaghan PW., Hussein M., Probert SD., "Multi-Vane Expanders as Prime Movers for Low-grade Energy Organic Rankine-Cycle Engines," Applied Energy, 16(2): 129–146 (1984).
[13] Badr O., O'Callaghan PW., Probert SD., "Multi-Vane Expander Performance: Breathing Characteristics," Applied Energy, 19(4): 241–271 (1985).
[14] Badr O., Probert SD., O'Callaghan P.W., "Multi-Vane Expanders: Vane Dynamics and Friction Losses," Applied Energy, 20(4): 253–285 (1985).
[15] Badr O., O'Callaghan PW., Probert SD., "Multi-Vane Expanders: Geometry and Vane Kinematics," Applied Energy, 19(3): 159–182 (1985).
[16] [16] Badr O., Probert SD., O'Callaghan PW., "Multi-Vane Expanders: Internal-Leakage Losses," Applied Energy, 20(1): 1–46 (1985).
[17] Badr O., Probert SD., O'Callaghan PW., "Performances of Multi-Vane Expanders," Applied Energy, 20(3): 207–234 (1985).
[18] Badr O., Probert SD., O'Callaghan PW., "Influences of Vane Design and Lubricant on a Multi-Vane Expander's Performance," Applied Energy, 22(4): 271–298 (1986).
[19] Badr O., Probert SD., O'Callaghan PW., "Optimal Design and Operating Conditions for a Multi-Vane Expander," Applied Energy, 24(1): 1–27 (1986).
[20] Badr O., Probert D., O'Callaghan PW., "Selection of Operating Conditions and Optimisation of Design Parameters for Multi-Vane Expanders," Applied Energy, 23(1): 1–46 (1986).
[21] Van Antwerpen HJ., Greyvenstein GP., "Use of Turbines for Simultaneous Pressure Regulation and Recovery in Secondary Cooling Water Systems in Deep Mines," Energy Conversion and Management, 46(4): 563–575 (2005).
[22] Wei D., Lu X., Lu Z., Gu J., "Performance Analysis and Optimization of Organic Rankine Cycle (ORC) for Waste Heat Recovery," Energy Conversion and Management, 48(4): 1113–1119 (2007).
[23] Tournier JM., El-Genk MS., "Axial Flow, Multi-Stage Turbine and Compressor Models," Energy Conversion and Management, 51(1): 16–29 (2010).
[24] Yang B., Peng X., He Z., Guo B., Xing Z., "Experimental Investigation on the Internal Working Process of a CO2 Rotary Vane expander," Applied Thermal Engineering, 29(11-12): 2289–2296 (2009).
[25] Nickl J., Will G., Quack H., Kraus WE., "Integration of a Three-Stage Expander into a CO2 Refrigeration System," International Journal of Refrigeration, 28(8): 1219–1224 (2005).
[26] Subiantoro A., Ooi KT., "Analytical Study of the Endface Friction of the revolving Vane Mechanism," International Journal of Refrigeration, 34(5): 1276–1285 (2011).
[27] Shen YT., Hwang YR., "Design and Implementation of an Air-Powered Motorcycles," Applied Energy, 86(7-8): 1105–1110 (2009).
[28] Huang K.D., Quang, KV., Tseng, K.T., "Study of Recycling Exhaust Gas Energy of Hybrid Pneumatic Power System with CFD", Energy Converstion Management., 1271-1278 (2009).
[29] Motor Development International (MDI) Home Page. Available online: http://www.mdi.lu/english/index.php (accessed on 8 March 2013)
[30] Koca A, Bayındır R, Gunes H, Kunt MA, Sakar S., "Design and Application of Electromagnetic Solenoid for Valve Mechanism on Compressed Air Engines", J Fac Eng Arch Gazi Univ, 26:73-79 (2011).
[31] Güneş, H., "Bir pnömatik motor kontrol sisteminin teorik ve deneysel analizi", Doktora Tezi, Gazi Üniversitesi Fen Bilimleri Enstitisü, Ankara 21-25 (2012).